

## Monte Carlo Simulation of a Catalytic Surface: Activity and Selectivity of $\gamma$ -Alumina for Dehydration

JOHN E. DABROWSKI, JOHN B. BUTT,\* AND HARDING BLISS

*Department of Engineering and Applied Science, Yale University,  
New Haven, Connecticut 06520*

Received August 12, 1969

The acidic properties and catalytic activity of oxide surfaces have been shown in a number of cases to be directly influenced by their degree of hydration. In the present work the rates and selectivities of ethanol dehydration on a well characterized gamma alumina have been measured experimentally over the temperature range of 180 to 400°C with feeds containing 0, 10, 20, and 40 mole % water. The effects of surface hydration and feed composition are compared with the predictions of a Monte Carlo simulation based on a model of the alumina surface and the mechanism of the dehydration reaction. The simulation is in good agreement with experiment, and points clearly to the distinctions which can be made between the separate effects of reaction energetics and surface configurations on rate and selectivity in the reaction.

### INTRODUCTION

The acidic properties and catalytic activity of oxide surfaces have been shown in a number of cases to be influenced by their degree of hydration. In the case of alumina, which is the subject of this study, data on these effects have been reported by Hindin and Weller (1), Pines and Haag (2), MacIver *et al.* (3), Hall *et al.* (4) and Myers (5), among others. A further problem when these oxides are catalysts in dehydration reactions is that the product water will also affect the nature of the catalytic surface. This interaction is more complex than simple adsorption competition or product inhibition, since the intrinsic activity or selectivity is altered.

The general purpose of the present work was to study these coupled effects in a simple dehydration reaction both experimentally and with simulation methods based on postulates of the catalytic surface and the reaction mechanism. The specific system employed—ethanol and  $\gamma$ -alumina—

is familiar but hopefully not shopworn. While the ethanol reaction is not a general example of the class of alcohol dehydration reactions, the general aspects of the mechanism of its dehydration on alumina are agreed upon and the reaction demonstrates both activity and selectivity (diethyl ether or olefin formation) properties which are susceptible to alterations in the catalytic surface—desirable for the purposes of this study. In addition, simulation techniques similar to those employed here have previously been successfully employed in studies of the hydration of the  $\gamma$ -alumina surface.

### THE CATALYST AND ITS SURFACE

The unit cell of the gamma phase of alumina, which is in crystalline structure a tetragonally deformed spinel (6), consists of 32 oxide ions, which correspond to  $21\frac{1}{3}$  aluminum ions distributed in octahedral and tetrahedral positions. The “sandwiching” of aluminum ions between oxide planes of close packing apparently causes the characteristic lattice distortion of alumina. Details of the crystallography of alumina are given at length by Lippens (7).

\* Present address: Department of Chemical Engineering, Northwestern University, Evanston, Ill. 60201.

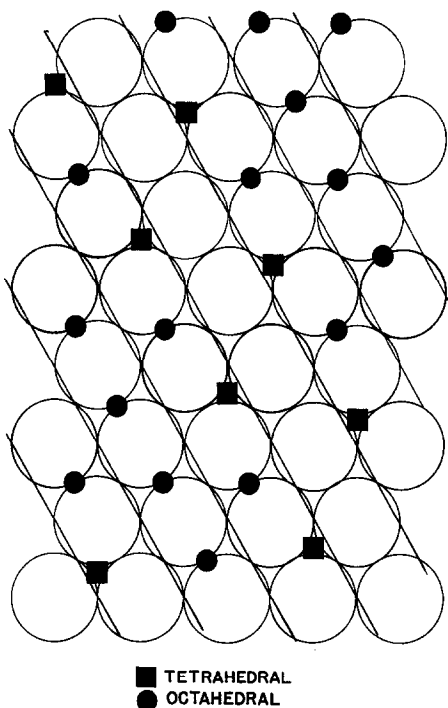


Fig. 1. Gamma alumina surface, (100) plane.

The preferentially exposed (100) surface plane (7) consists of parallel rows of oxide ions which are the edges of the oxide planes of closest packing, shown along the solid diagonal lines of Fig. 1. This surface schematic is constructed from the two alternately stacked layers of alumina described by Lippens and is the projection of the (100) surface on a plane perpendicular to that of closest packing. Since the surface is considered to terminate in anions (oxides and hydroxides) (8), the outermost aluminum ions are below the surface plane. These aluminum ions provide the electrophilic centers by which water is held on the surface; hydration occurs dissociatively, with the electron pair of the hydroxide being positioned over the aluminum ion while the dissociating proton forms a hydroxyl via binding to lattice oxygen (9). The resultant lattice hydroxide is positioned on the surface below the plane of the parent hydroxide. It is reasonable to expect differences in the energies of interaction for octahedrally and tetrahedrally coordinated aluminum ions, although such information is not available.

The picture of the surface and the specific interactions involved in its hydration follows the prior treatment of Peri (10-11), who employed a Monte Carlo simulation to identify the types of surface site configurations resulting from the dehydration of a fully hydrated surface. This type of dehydration may be equated with thermal treatment of the alumina, and in our subsequent analysis the temperature level can be taken to define a degree of surface hydration. While the surface and hydration models employed are idealized to the extent of ignoring factors such as surface defect structure or energy distribution, the previous success of entirely analogous procedures employed by Peri for structural interpretation of spectral data on the hydrated alumina surface provides some justification for the general approach. Similar methods have been employed successfully by Callahan and Grasselli (12) for predicting selectivity in propylene oxidation with metal oxide catalysts as a function of the oxidation state of the catalytic surface.

#### THE REACTION SYSTEM

The details of alcohol dehydration reactions on alumina have been summarized by Winfield (13) and, more recently, by Pines and Manassen (14) and the major aspects of their mechanisms seem clear at this point. Most postulates of mechanism for ethanol dehydration are keyed to the existence of a chemisorbed ethoxide on the alumina surface, which results from dissociative chemisorption of the alcohol yielding an ethyl group chemisorbed on the catalyst oxygen. Various proposals have been made regarding the manner in which the ethoxide participates in the surface reaction, since a selectivity between diethyl ether (favored at low temperatures) and ethylene (favored at high temperatures) is involved. Various points of view are represented in the recent literature:

- (i) Ether production by interaction of two adjacent ethoxides (15); olefin production by internal degradation (hydrogen

abstraction) in conjunction with adjacent oxides (15, 16).

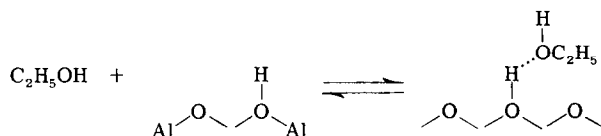
(ii) Same as (i) except ether production via a Rideal type mechanism involving one ethoxide and one ethanol (17).

(iii) Ether formation through the reaction of a surface ethoxide group with a nearby molecularly adsorbed alcohol (18).

(iv) Ethylene formation by means of a

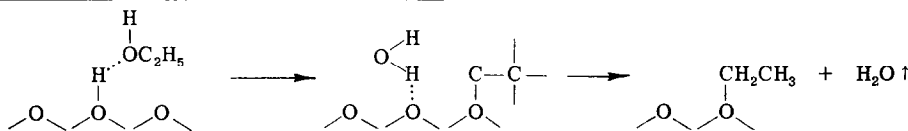
trasting processes represented in (i) and (iv) above are discussed in Refs. (16) and (19), respectively, and while the issue cannot be considered resolved we feel that the bulk of evidence to date supports (i). The detailed sequence of the reaction may then be written as follows:

1. Weak adsorption of ethanol:



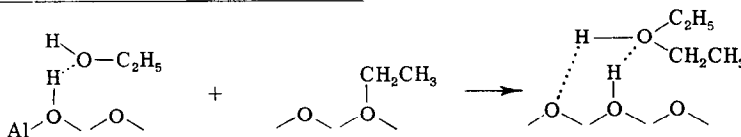
concerted mechanism requiring paired acid-base sites; ether formation as in

2. Chemisorption of the weakly-adsorbed ethanol:



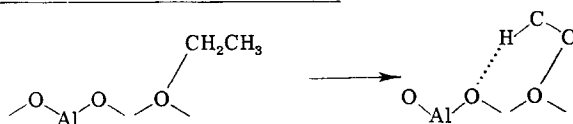
(iii), (19).

3. (a) Ether formation:



While the above is not a complete re-

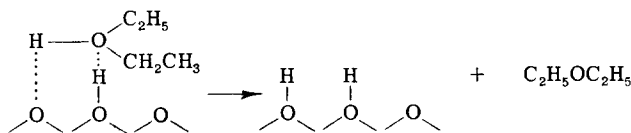
(b) Ethylene formation:



view, the mechanistic possibilities are comprehensive. The participation of two

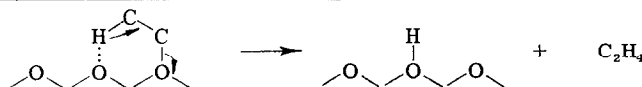
(product of reaction 2)

4. (a) Desorption of ether:



adjacent ethoxides in ether production is

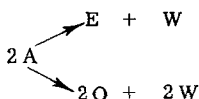
(b) Desorption of ethylene:



unlikely, since formation of ether is favored by the hydrated surface (lower temperatures). On the other hand, discrimination between the two modes of ethylene formation on this basis is not possible. The con-

In our subsequent discussion it will be convenient to view this sequence in terms of separate energetic and configurational factors. The former refers specifically to the energy requirements involved in the

making and breaking of bonds, while the latter pertains to the location of chemisorbed species on the catalyst surface. The elementary step of 3(a) postulates, for example, that an alkoxide complex must be adjacent to a weakly-adsorbed ethanol for ether formation to occur. The particular value of simulation techniques such as the Monte Carlo method used in this work is that such configurational effects on the rate of reaction may be clearly separated from the other contributing mechanistic effects. The overall reaction of steps (1)–(4) above may be represented by the following kinetic scheme (20, 21) at low conversions:



#### THE MONTE CARLO MODEL AND ITS IMPLEMENTATION

The preferentially exposed (100) plane of  $\gamma$ -alumina is considered to be the surface of interest. The equivalent octahedrally placed aluminum ions depicted in Fig. 1 are fixed in location; these ions constitute 19 of the  $21\frac{1}{3}$  total in the unit cell. The two remaining aluminum ions which occur within tetragonal positions may be placed in any of five locations, and their behavior is different from the octahedral ions as described below.

**Hydration.** In Fig. 2 is given an enlargement of a section of the surface of Fig. 1. Hydration via dissociative chemisorption in the octahedral case is straightforward; the OH attaches directly above the aluminum (H in Fig. 2) while the remaining proton attaches to an adjacent surface oxide. Hydration over tetrahedral aluminum is somewhat more complicated since the OH may adsorb over either of two equivalent positions which are equidistant from the aluminum. These equivalent positions lie along the close packed plane and are represented as E in Fig. 2. The choice of positions for the OH must be random and the point of deposition of the proton is dependent on the position selected for the OH. Although a distinction

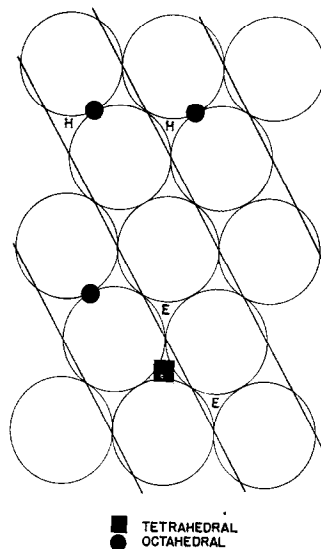


FIG. 2. Detail of gamma alumina surface.

between the two differently coordinated aluminum ions is made here, they are treated equivalently in the computations of the simulation.

**Adsorption.** Adsorption of reactants on the hydrated surface occurs as shown in the mechanistic picture (steps 1 and 2), on the OH of hydration, that is, on the outermost layer of hydroxyls. The OH formed from the dissociated proton and lattice oxygen is postulated not to be active in adsorption since, to the extent of detail available on the system its inclusion would not affect the results of the simulation, but would increase the computational effort. The competitive adsorption between ethanol and water is of particular interest to some of the experiments of this study run with feed mixtures of alcohol and water. We define a competitive adsorption modulus  $K$ .

$$K = \left( \frac{\theta_A}{\theta_w} \right) \left( \frac{P_w}{P_A} \right) \quad (1)$$

where  $\theta_A$ ,  $\theta_w$ ,  $P_A$  and  $P_w$  are the surface coverages and partial pressures of alcohol and water, respectively. Some experimental data on adsorption competition have been reported by Kipling and Peakall (23), who measured at room temperature a chemisorption ratio of 0.26 between ethanol

and water on  $\gamma$ -alumina. A similar magnitude of this ratio is also obtained from the results of an earlier study of the kinetics of the dehydration reaction in this laboratory (20). Those data, in the temperature range 274–314°C, indicate a temperature dependence of  $K$  corresponding to an activation energy of only about 3 kcal/mole. An approximate calculation based on the assumption that the relative rates of desorption of the two species are proportional to their dipole moments while relative rates of adsorption are given by standard kinetic theory corrected for steric hindrance of the alkyl group in ethanol gives a value of approximately 0.3 for  $K$  (22), while Kipling and Peakall arrive at a value of 0.33 from strictly geometric considerations. It thus appears a reasonable first approximation to consider  $K$  constant and independent of temperature (based on relative magnitudes of reaction and adsorption energetics); the following analysis presents results for  $K = 0.3$ .

**Simulation.** The configurational requirements for the two reaction paths available to the ethoxide determine, in part, the extent and selectivity of the overall reaction. These factors are evaluated in the simulation. The surface is described as a planar oxide matrix to which aluminum ions and water (as H and OH) have been added; each oxide is treated as a member of an array cataloged by row (i) and column (j). The elements in the array are stored as identifying symbols, for example E for ethanol and O for oxide. Relative positions of the elements may thus be examined by printing a portion of the stored array. Since the output occurs in fixed printer positions, the actual relative distances between surface elements must be kept in mind. The elementary unit of surface in the simulation contains 32 oxides and to facilitate analysis, operations on the total matrix (about 100 000 positions) consist of the summation of operations on single rectangular  $4 \times 8$  units positioned in the matrix. Edge effects are eliminated by treating the surface as two cylinders, the last column adjacent to the first and the

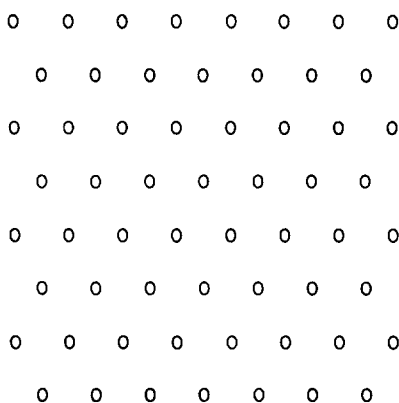


FIG. 3. Basic oxide array.

top adjacent to the bottom for all matrix operations. A typical output of a portion of the oxide array is given in Fig. 3.

Within the oxide matrix aluminum ions are distributed into the octahedral positions in accordance with the geometry of Fig. 1. The placement of tetrahedral aluminum, however, is subject to some complications since there are five equivalent tetrahedral positions within the unit cell of  $\gamma$ -alumina, two of which may be occupied to provide the total aluminum required. The procedure devised (22) for generation of the final alumina surface utilizes each of the five tetrahedral positions an equal number of times; results for the aluminum oxide array are given in Fig. 4.

Hydration of the surface to a specified degree is carried out in two steps, placing

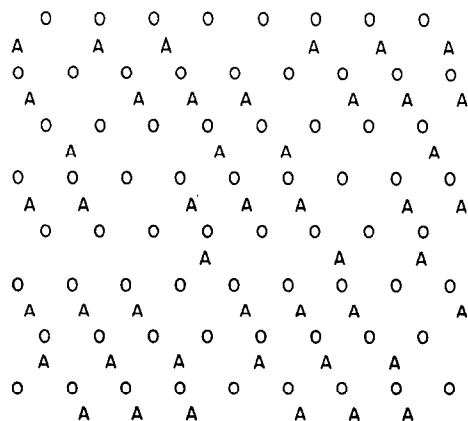


FIG. 4. Aluminum oxide surface: A = aluminum; O = oxygen.

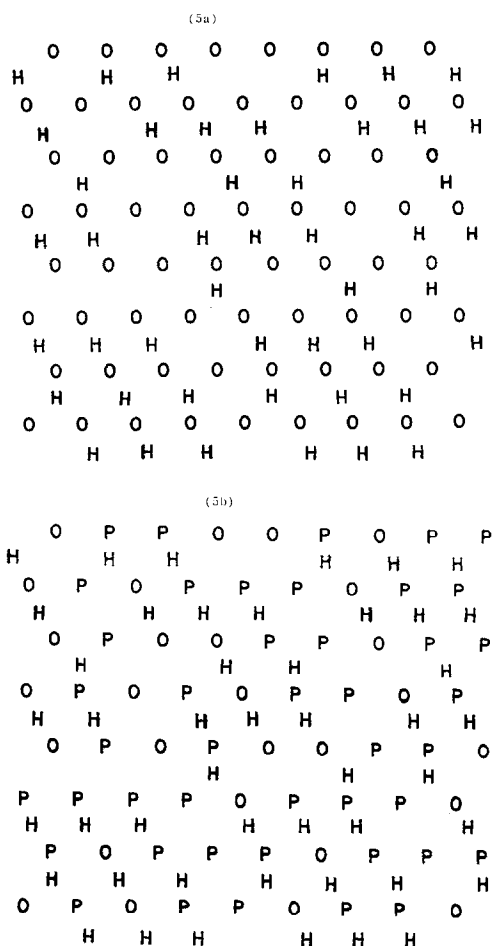


FIG. 5a. Surface after placement of hydroxyls: O = oxygen; H = hydrated site; (b) hydrated surface with protons emplaced: P = oxygen site plus proton.

OH and H, respectively. In order to ensure surface hydration as randomly as possible, the following procedure is used. A vector consisting of 16 000 elements is hydrated to the specified degree for the surface by systematically storing within it H for hydration or blank for no hydration. Then a number is selected from a random number table (between 1 and 16 000) to provide the address of a single element of the vector which is the site to be hydrated. The hydration is accomplished symbolically for both octahedral and tetrahedral sites by replacing the A with an H. The proton from the dissociated water of hydration is placed on the lattice oxide to complete the

hydration procedure; in this step P replaces O of the lattice. Note that at 100% hydration, the alumina surface is not comprised of only hydroxyl groups. Since there are 21 aluminum ions for each 32 oxide ions and since each molecule of water converts a single surface oxide to a hydroxyl, there remain eleven surface oxides at 100% hydration. Such a fully hydrated surface is depicted in Fig. 5a and b.

The chemisorption of reaction mixture on the surface is carried out by specifying the surface composition according to the degree of hydration and the reactant composition. For competitive adsorption between ethanol and water the modulus of Eq. (1) is employed with feed composition to then specify relative amounts on the surface. This composition information forms another vector from which the random number table selects the addresses of various adsorbed characters. The results for the adsorption of a reaction mixture containing 40 mole % water and 60 mole % ethanol on the hydrated surface of Fig. 5b are shown on Fig. 6, where E denotes adsorbed ethanol and W, adsorbed water.

Now a logical search is performed on the surface array of Fig. 6 to determine the locations of a lattice oxide adjacent to a sorbed ethanol; upon locating this configuration an ethoxy "complex" is formed on the oxide site. Symbolically the complex formation is represented within the

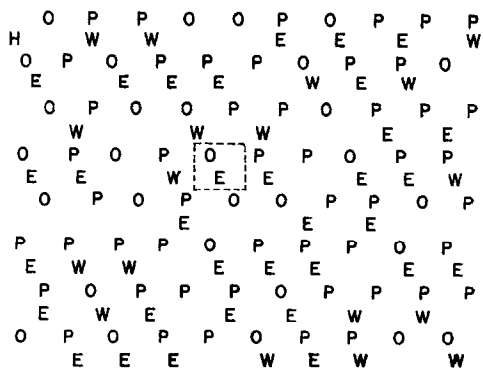


FIG. 6. Reaction mixture (60% ethanol, 40% water) adsorbed on surface: E = adsorbed ethanol; W = adsorbed water; enclosure contains configuration for complex formation.

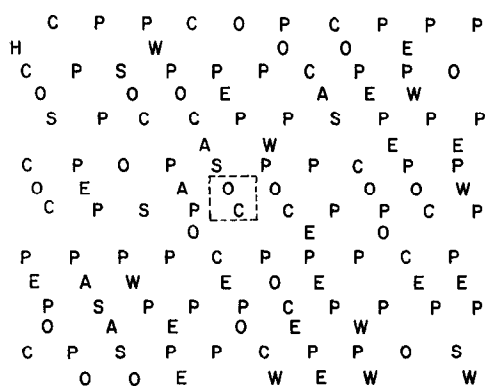


FIG. 7. Formation of ethoxy complex on surface: C = ethoxide complex; S = site hydrated by adsorbed water.

array by writing C over the O involved, and replacing the E with O. Note that the latter operation also signifies the desorption of water from the catalyst surface during complex formation, as per reaction 2 of the mechanism. The result of this search is given in Fig. 7.

The formation of products, that is, the actual surface reaction, is determined by search of the matrix of Fig. 7. For ether formation the search is conducted by locating a surface complex and testing the elements around this location for weakly chemisorbed ethanol (E). If ethanol is found adjacent to the complex, the register counting favorable configurations is singly incremented, otherwise the unfavorable register is incremented. Ethylene formation is treated analogously to ether formation; for ethylene, however, the complex location adjacent to an oxide (which can receive the proton abstracted in its formation) is favorable.

**On randomness.** To maintain as random a total event composed of several subordinate events, only one subordinate event may be random. For simulation of surface hydration, complete randomness in the selection of the sites to be hydrated is necessary. For 90% hydration, for example, it is not sufficient to permit every tenth site of the entire surface to be blank, certainly. Rather we select elements from the "hydration vector" consisting of 90% H and 10% blank and deposit them on the ordered

oxide surface of Fig. 4. The randomness in the so-far ordered total event is introduced by selecting the elements from the hydration vector in a random fashion. For competitive adsorption a similar procedure is used. An ordered column vector is established with the desired adsorbate composition (determined from the feed composition and the computed relative adsorption modulus) and an ordered search of the surface for adsorption sites is conducted; randomness is introduced by selection from the vector based on the random number table.

#### RESULTS OF THE SIMULATION

While the simulation cannot be used to calculate absolute quantities, relative values of "configurational favorability" with respect to some known condition are sufficient to predict trends in activity and product distribution. The effect of two parameters, degree of surface hydration and reaction mixture composition, can be investigated straightforwardly via the simulation. Since the state of hydration of  $\gamma$ -alumina is determined by its temperature, changes in product distribution with surface hydration are an indirect measure of the temperature effect on configuration. Energy requirements, however, determine the fraction of favorable configurations which actually become products. At a set temperature level, activity and selectivity variations with feed composition are simulated directly in terms of the adsorption competition and configuration calculations. Energy factors remain constant at the set temperature, and thus do not enter into the calculations.

Some example results of the determination of product formation configurations are given in Table I as a function of degree of surface hydration and feed composition. Since the surface is of fixed size in all simulations, the comparison of surface configurations under these differing conditions is valid. In Table Ia, for example, at 100% surface hydration the average number of favorable configurations for ether formation with 0% water in the feed is 1618, while for 10% water it is 932. Thus, the

TABLE 1a  
EXAMPLE MONTE CARLO RESULTS FOR  
CONFIGURATIONAL FAVORABILITIES

Degree of surface hydration (%)	Water in feed (%)	Av. no. of favorable configurations for formation		No. of Monte Carlo expts.
		Ether	Olefin	
100	0	1618	3004	10
	10	932	2317	10
90	0	1340	3272	3
	10	801	2528	3
80	0	1062	3470	3
	10	592	2633	3
70	0	786	3441	3
	10	441	2657	3
60	0	503	3350	3
	10	296	2556	3
50	0	304	3038	3
	10	177	2331	3
40	0	173	2649	2
30	0	59.5	2106	2
20	0	13.5	1481	2
10	0	4	770	2
0	0	0	0	2

<sup>a</sup> Based on a surface oxide matrix consisting of approximately 100 000 storage locations with the simulation performed in five steps as in Figs. 4-7.

TABLE 1b  
EXAMPLE OF VARIATION IN MONTE CARLO  
RESULTS FOR A GIVEN SIMULATION  
Degree of surface hydration = 100%.

Trial	0% Water in feed		10% Water in feed	
	Ether	Olefin	Ether	Olefin
1	1630	3031	957	2296
2	1612	3032	894	2304
3	1613	2954	928	2327
4	1599	3031	912	2336
5	1607	3007	909	2302
6	1654	3019	906	2308
7	1631	2984	972	2345
8	1642	2996	941	2316
9	1591	2977	940	2330
10	1604	3010	964	2308

simulation indicates that the configurational favorability for ether formation in this case is reduced to (932/1618) or 0.576 of the value for pure ethanol. Since this refers to a fixed temperature, the number

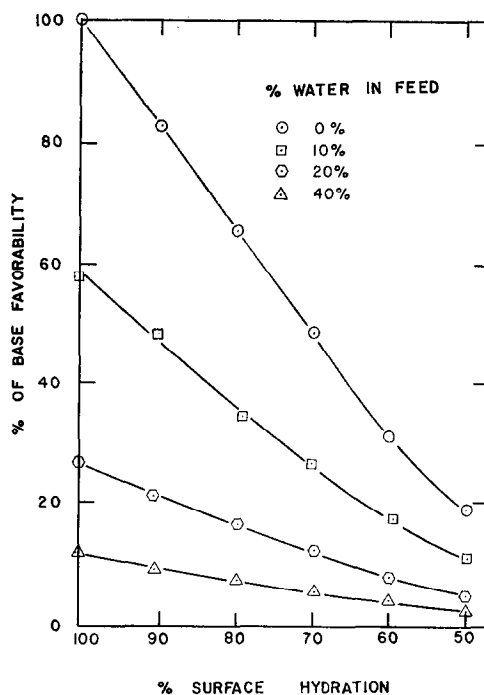


FIG. 8. Effect of surface hydration on ether formation; symbols indicate computed results from Monte Carlo simulation.

is directly translatable into relative rates of reaction and affords an immediate comparison with experiment, as shown below.

#### Effect of the degree of surface hydration.

At surface hydration levels less than the fully hydrated state the average distance between adsorbed reactants increases and the configurational favorability for ether formation decreases. Figure 8 illustrates the predicted effect of the degree of surface hydration on the reactive favorability for ether formation with various feed mixes. The ratios shown are with respect to the favorability for ether formation on the fully hydrated surface and appear to decrease monotonically with decreasing surface hydration.

For ethylene formation, on the other hand, a maximum is found in the hydration-favorability correlation, as shown on Fig. 9. In this case although the hydroxyl sites decreased as surface hydration is decreased the number of oxides increase correspondingly, and since oxide sites are necessary for the hydrogen abstraction of

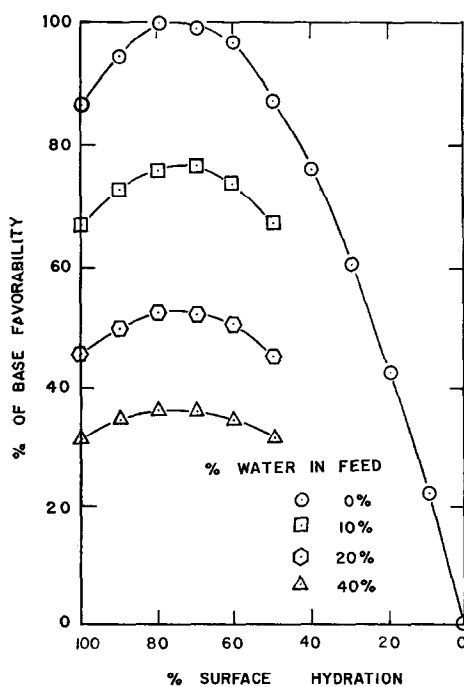


FIG. 9. Effect of surface hydration on ethylene formation; symbols indicate computed results from Monte Carlo simulation.

reaction 3(b) an increase in relative favorability over a small range of decreasing hydration is reasonable. The ratios shown in Fig. 9 are with respect to the maximum favorability computed, corresponding to a surface hydration of 80% and pure ethanol reactant. It is interesting to note that the simulation predicts substantial favorabilities for ethylene formation on the fully hydrated surface, corresponding to lower temperatures. This is not detected experimentally, the reason being the energy requirement for this reaction.

#### Effect of reaction mixture composition.

The adsorption competition between ethanol and water can also alter reaction behavior. Water in the feed produces a decrease in favorability for both ether and ethylene formation compared to pure ethanol reactant, and the simulation indicates a more pronounced effect on ether. The computed variations as a function of reactant composition are shown on Fig. 10 where the ratios are evaluated differently than in Figs. 8 and 9. In Fig. 10 the per-

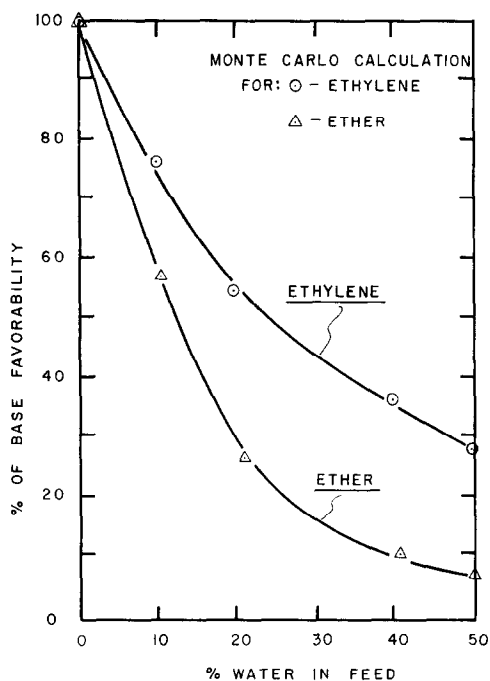


FIG. 10. Effect of feed composition on relative favorabilities for ether and ethylene formation.

centages of base favorability relative to that for pure alcohol feed at the same degree of hydration are plotted. The effect of this normalization procedure is to eliminate surface hydration as a distinguishable variable, i.e., the simulation indicates that relative rate effects due to adsorption competition are independent of surface hydration. As shown, ether formation is inhibited to a considerably larger extent than ethylene by the presence of water.

#### EXPERIMENTAL MEASUREMENTS

The experiments were designed to permit observation of the effects of water content of the feed stream and degree of hydration of the catalyst on rates of reaction and selectivity, the variables capable of description with the Monte Carlo method, so that comparisons between the two could be made. Details are reported by Dabrowski (22).

#### Catalyst preparation and pretreatment.

Gamma alumina was made according to the recipe of MacIver, *et al.* (26). The

gelatinous boehmite was dried at 120°C, heated to 500°C in a muffle furnace, ground, sieved, and a 30–270 mesh (U. S. Sieve series) was selected. The crystalline structure was verified with X-ray analysis and comparison with the data of Lippens (7). BET area was determined to be 206 m<sup>2</sup>/g. The catalyst was stripped of any extraneous volatile material by passing over it a stream of dry nitrogen at 200°C to constant weight. Such stripping was continued for 24 hr at reaction temperature after the catalyst was introduced into the reactor. Subsequent hydration of the catalyst is described below.

**Reaction system.** Alcohol (sometimes containing water) was fed from a constant head tank, purged with nitrogen, through a rotameter and a vaporizer to the reactor. Temperature in the vaporizer was not permitted to rise above 130°C to insure absence of catalytic effects of stainless steel. Stainless steel tubing leading from the vaporizer to the reactor was kept at about 100°C in a simple stirred air bath.

The reactor consisted of a 1-in. i.d. Kimax U-tube, one leg of which, serving as a preheater, was packed with 3/8-in. glass rings and heated externally with tapes. The catalyst, supported on glass wool was in the other leg. Capillary wells were provided to hold chromel–alumel thermocouples with junctions at the center line. The amount of glass wool could be varied so that the middle of the catalyst bed (which was also varied in weight) could be aligned with the thermocouple well center. Sampling ports were placed before and after the U-tube. The entire reactor was immersed in a fluidized sand bath (Type SBL-2, Techne, Inc., Princeton, N. J., with a modified temperature control).

The product gas from the reactor was sent to waste. The feed could be diverted to a condenser-receiver for measurement of its rate.

**Adsorption experiments.** A model RG Cahn electrobalance was used for a series of isobaric water adsorption measurements. The “hangdown” tube was specially provided with a heated tee through which nitrogen containing known amounts of

water vapor could be introduced in a downward direction. Two Teflon baffles (restricting the cross-section to about 1/10 the open area) were introduced above the tee to minimize diffusion of water vapor toward the balance mechanism. In addition a dry nitrogen stream was introduced through the center tube near the mechanism to flow through the baffle holes. The leg between the baffles was heated with an infrared lamp. This arrangement prevented condensation of water on the system components at ambient temperature. For the isobaric measurements the equilibration of the sample was with dry nitrogen in all cases. Temperature control was maintained with a jacket furnace fitted around the hang-down tube. A thermocouple was sealed into this tube near the bottom and extended to 1/4 in. below the balance pan. The hang-down tube below the furnace led to a tee (heated with an infrared lamp) and to a sampling port.

**Analysis.** Analysis of the products was accomplished with an F and M Scientific Co. Model 700 gas chromatograph in series with a Perkin-Elmer Model 154. The F and M, with a 2-m column of 10% Carbowax 20M on Haloport F, separated air-ethylene, ether, ethanol, and water at 80°C. Helium carrier gas flow rate was 50–60 ml/min and pressure was 15 psig. A Dry Ice–acetone bath was provided between the two chromatographs so that only air and ethylene were separated in the second. The second column, operated at 90°C, was packed with 2 m of silica gel.

**Procedure (rate measurements).** After the desired reaction temperature was attained in the sand bath, dry nitrogen was passed over the catalyst for 24 hr. During this period the liquid feed was started and the vaporizer heater was adjusted so that the vapor temperature was about 120°C. The feed vapor was vented until the beginning of a run. The run proper was begun by switching from the nitrogen purge to the alcohol–water feed. The first samples of feed and of product were taken after 2 hr had elapsed; usually about five samples were taken. Prior to sampling, the temperature of the catalyst was measured.

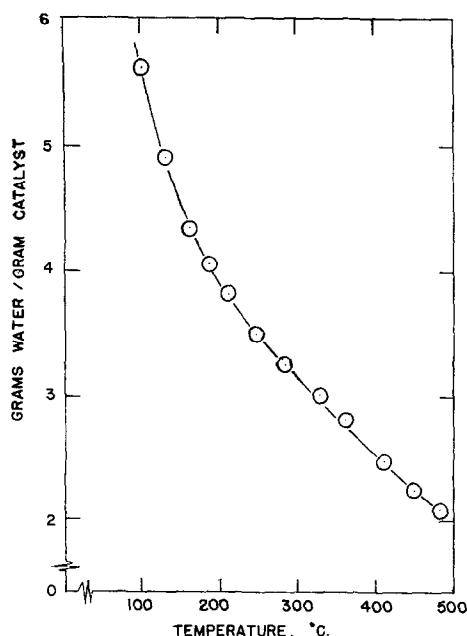


FIG. 11. Adsorption isobar for water on gamma alumina; equilibration in dry nitrogen at 1 atm.

After sampling, the exact flow rate of the feed in each run was determined by diverting it to the condenser-receiver section in which the rate of weight accumulation was observed. The product flow rates were not measured. In a few runs the catalyst was preconditioned by passing over it nitrogen from the saturator containing water vapor of known partial pressure.

**Procedure (adsorption measurements).** Isobaric desorption measurements were made with 594 mg of catalyst by passing dry nitrogen over it at room temperature until a constant weight was attained. The temperature was then increased and a new value of constant weight was attained, normally within 24 hr. This procedure was continued in steps to 485°C. The water content of the final sample, desorbed at 485°C, was determined by measuring further weight loss after calcining the sample at 1200°C.

**Absence of gradients.** The absence of boundary layer gradients was assured by making a few runs at variable flow rates at 220.8°C. The conversion (less than 3%) varied linearly with flow rate, character-

istic of the absence of significant boundary layer effects. An independent calculation according to the method of Yoshida *et al.* (24) verified this conclusion.

The effect of intraparticle diffusion was not checked experimentally, but a calculation according to the method of Weisz and Hicks (25) showed this to be unimportant. Furthermore, prior studies (17) in this laboratory with the same system have shown this effect unimportant under conditions far more severe than those employed in the present study.

Blank runs were made at 400°C with pure ethanol feed to check the catalytic properties of the reactor system itself. Under no conditions was a conversion greater than 0.1% noted, a negligible quantity compared to those determined in experimentation with the catalyst.

#### EXPERIMENTAL RESULTS

**Adsorption studies.** The results of the isobaric measurements are shown on Fig. 11. Such desorption (above the 200 to 200°C range) should be visualized as simple surface dehydration arising from the random combination of adjacent hydroxyl groups to form water which is removed (10). As Fig. 11 demonstrates, this dehydration is a function of temperature, the level of dehydration increasing with temperature. The present results are consistent with those reported by MacIver, *et al.* (26) and support their contention that there is excess water on the gamma alumina surface which is not eliminated until temperatures in the 200–300°C range are attained. Thus, at and below these temperatures the surface may be considered fully hydrated. We will attempt later to define this limiting temperature of complete hydration more closely.

**Initial reaction rates.** Initial rates of dehydration were measured at temperatures from 173 to 400°C using the catalyst described previously and with feed compositions ranging from 0 to 40 mole % water. Feed rates were varied from 0.16 to 0.86 g/min.

The products observed were entirely ether and water below about 245°C. Above

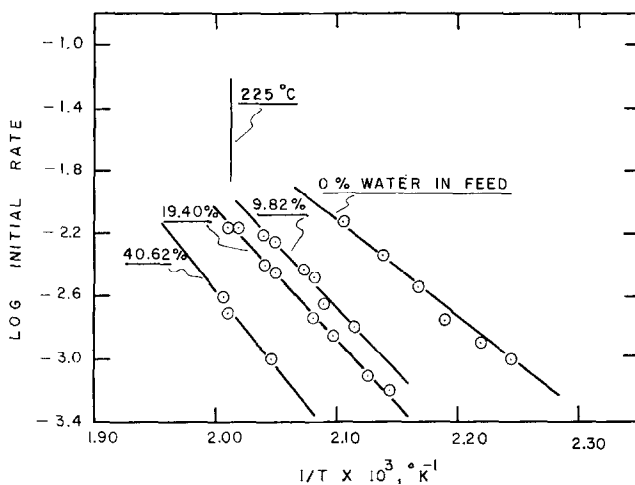


FIG. 12. Initial rates of ether formation for various feed compositions in the temperature range below 225°C

this point ethylene appeared, but did not predominate until about 360°C; ether was present even at the highest temperatures. Conversions were maintained below about 7% for ether and 3% for ethylene, consistent with initial rate analysis. Absolute values of the experimentally determined initial rates are tabulated by Dabrowski (22). These data, in terms of the log initial rate in units of moles of alcohol reacted/100 g of catalyst/min, are also given in Figs. 12-17 of the following section.

#### COMPARISON OF THE SIMULATION WITH EXPERIMENTAL RESULTS

##### Reaction mixture composition effects.

The experimental data of interest here are the ratios of rates at any feed composition to those for pure alcohol feed at the same reaction temperature; these should be directly comparable with the Monte Carlo calculations, as discussed previously. The initial rate data obtained in the experimental investigation are given on Figs. 12-14 (ether formation) and Figs. 15 and

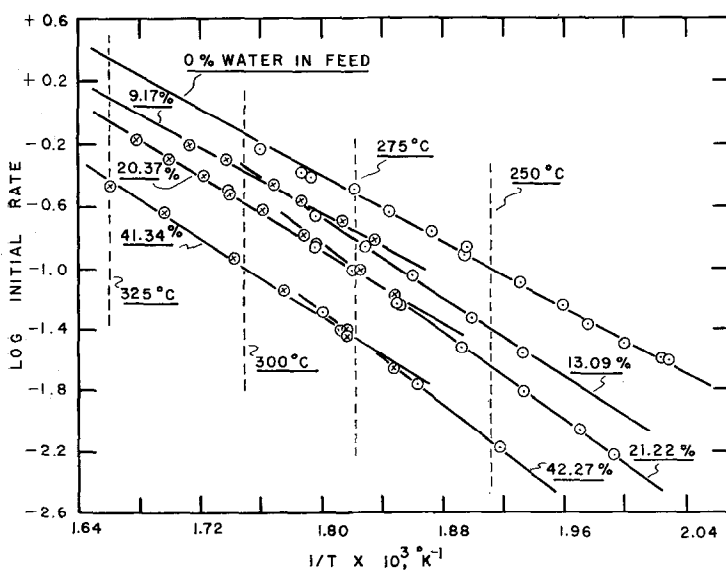


FIG. 13. Initial rates of ether formation for various feed compositions in the temperature range 225-325°C.

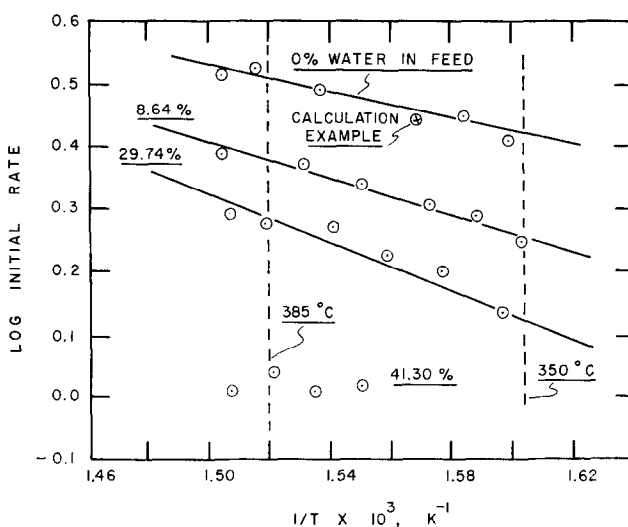


Fig. 14. Initial rates of ether formation for various feed compositions at temperatures above 325°C.

16 (ethylene formation) as a function of feed composition. Interpolation of these rate data has been carried out at the temperatures indicated by broken vertical lines on the plots and relative rates calculated from the interpolated values. The comparison of experimental rate ratios with those determined by the Monte Carlo simulation is shown on Fig. 17. In general the agreement seems quite reasonable, and

the data confirm that the effect of water in the feed is to inhibit ether formation to a greater extent than ethylene formation. There is some scatter at high water content in the data for relative rates of ethylene formation which is beyond the limits of experimental error. The reason for this is most likely due to variation in the competitive adsorption modulus  $K$ , which was taken to be independent of tem-

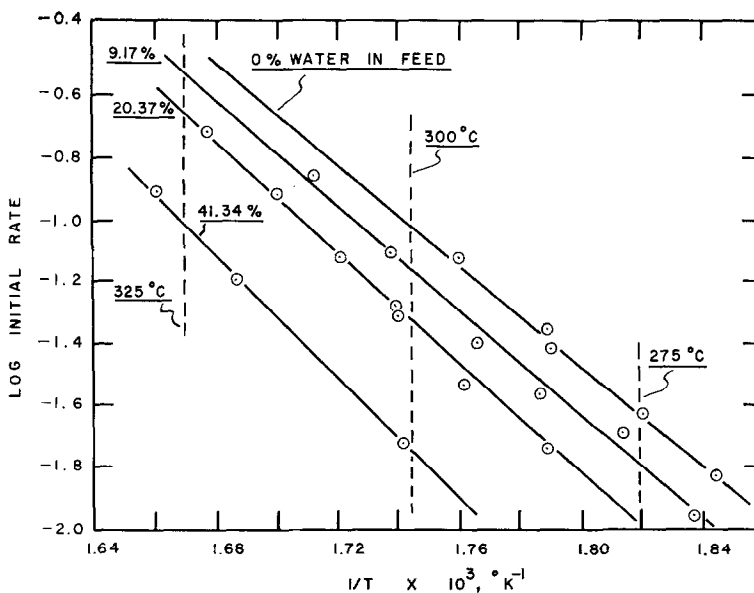


Fig. 15. Initial rates of ethylene formation for various feed compositions in the temperature range 275-325°C.

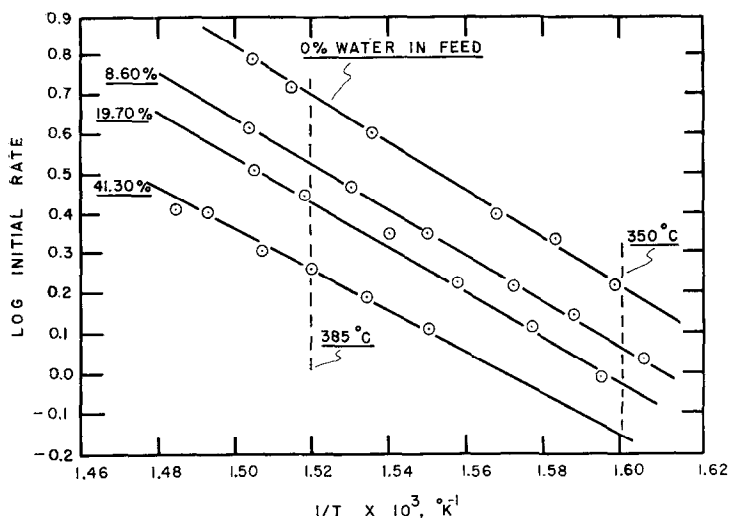


Fig. 16. Initial rates of ethylene formation for various feed compositions at temperature above 325°C.

perature and feed composition variation in the simulation. The temperature dependence, as discussed previously, does not appear to be large, but there could be significant interactions between ethanol and

water at higher water concentrations which alter the adsorption competition. There are, however, no independent data available on this point. The results also suggest the possibility of a selectivity toward preferential removal of the oxide sites necessary for ethylene formation under some conditions. Nonetheless, the results of Fig. 17 indicate over most of the range of variables that, for set temperature levels (i.e., energetic factors may be considered constant), good predictions of rate and selectivity variation with feed composition are available from the Monte Carlo simulation.

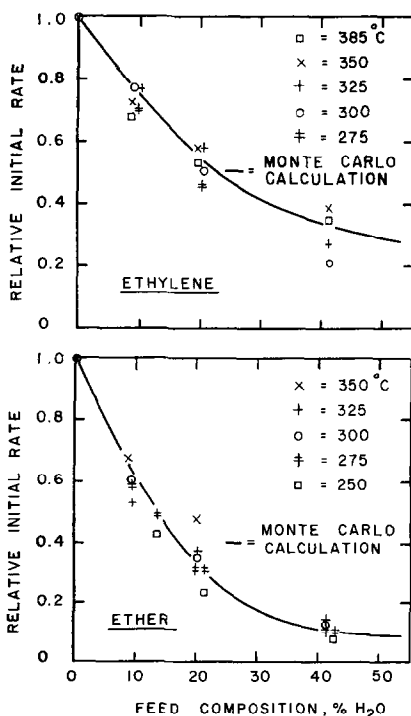


Fig. 17. Comparison of experimental initial rate ratios with those determined by Monte Carlo Simulation.

**Temperature dependence.** Before attempting to relate the temperature behavior of the reaction to the simulation in terms of surface hydration, it is necessary to describe this directly. Again, the pertinent rate data are given in Figs. 13–17 for both products. As seen, first of all, the Arrhenius-type plot cannot be represented by a single straight line over the entire range of temperatures investigated either for ethylene or for ether. The representation in terms of straight-line segments is arbitrary with the single exception of ether formation at low temperature, as discussed below.

The interpretation of reaction activation energies determined from the data on Figs. 13–17 is difficult since the nature of the

catalytic surface is changing in this temperature range. Values of the activation energy for ether formation at low temperatures are meaningful, however, because at these conditions the dehydration reaction is selective for ether and changes in the degree of hydration of the surface must be small, as discussed later. Values of activation energies for ether formation at differing water contents of the feed, determined from the data on Fig. 12, are given in Table 2. Over the range of temperatures

TABLE 2  
ACTIVATION ENERGIES FOR ETHER  
FORMATION ON THE HYDRATED SURFACE

Temp range (°C)	Water in feed (mole %)	$E'_a$ (kcal/g mole)
175-227	0	27.4
	9.82	34.5
	19.40	36.8
	40.62	44.6

where ethylene formation proceeds at a measurable rate some dehydration of the surface must occur and values of activation energy reflect this change as well as the energy requirements of the reaction. Such changes produce the deviation from linearity evident in Fig. 13. At comparable conditions of surface hydration, the apparent activation energies for ethylene formation can range up to several times greater than the corresponding values for ether; a brief summary of typical values is given in Table 3.

**Surface hydration.** Since the Monte Carlo simulation indicates that surface hydration

TABLE 3  
COMPARISON OF APPARENT ACTIVATION  
ENERGIES FOR ETHER AND ETHYLENE  
FORMATION UNDER CONDITIONS OF  
PARTIAL SURFACE DEHYDRATION

Temp (°C)	Water in feed (mole %)	$E_{app}$ (kcal/g mole)	
		Ether	Ethylene
300	0	24.3	36.6
	20.37	26.3	40.4
350	0	4.5	26.7
	19.74	7.8	26.4

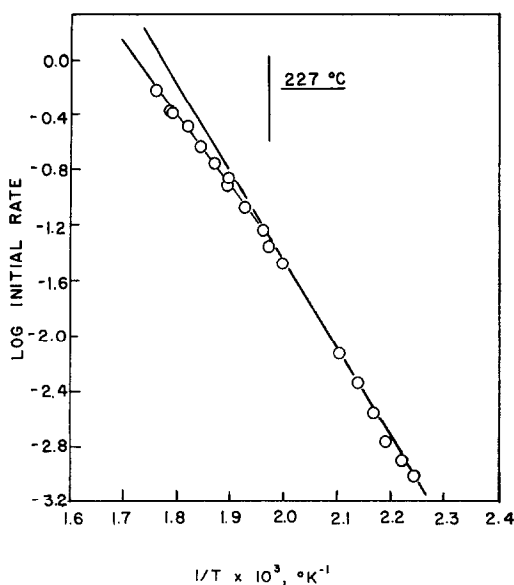


FIG. 18. Initial rates of ether formation in the temperature range from 175 to 287°C.

does not affect the product distribution or relative reactivities as a function of feed composition, an observation confirmed by the relative rate data of Fig. 17, such data do not permit the assessment of the absolute level of surface hydration or the description of how this is affected by temperature level. MacIver *et al.* (26) asserts that gamma alumina is fully hydrated at 200-300°C and that the water content at lower temperature (see Fig. 11) is "excess water."

A more detailed analysis of the effect of temperature on ether formation is illustrated in Fig. 18, where the logarithms of the initial rates of ether formation with no water in the feed versus reciprocal temperature are plotted. The temperature range is extended to 287°C; there is a clear break in this line at about 227°C (below which temperature the activation energy for ether formation was determined—Fig. 12). We confine our attention to the ether reaction, since no selectivity problems arise at low temperature; even at 287°C, ethylene formation is less than 10% of the total conversion. The ordinate of the lower (data) line at 287°C ( $1000/T = 1.77$ ) is  $-0.23$ , while that of the extended low temperature line is  $-0.02$ . Thus the

rate of ether formation at 287°C is 62% of what would have been expected on the basis of energetics alone. We attribute this reduction to the combination of partial surface dehydration and decrease in surface coverage. The amount of dehydration, determined experimentally, is given on Fig. 11 which shows a water content of the catalyst of 3.6 g/g at 227°C and 3.15 g/g at 287°C, a reduction of 13%. However, the observed 38% decrease in rate corresponds, according to the simulation calculations for pure alcohol feed, to a 20% dehydration of the surface.

**Surface coverage.** The discrepancy between the two values obtained for the extent of dehydration must be due largely to changes in surface coverage with temperature, which are not considered in the simulation. If the water content is reduced by 13%, the alcohol coverage should be reduced by the same value assuming the validity of the constant ratio of adsorption. The rate of reaction is approximately linear in surface coverage, so that 13% of the observed 38% decrease can be assessed to reduced coverage. The remaining 25% reduction, due to surface dehydration, corresponds to an extent of dehydration of 14% according to Fig. 8, which is in good agreement with the experimental result.

This type analysis can similarly be applied at higher temperatures, although the procedure is more complicated since ethylene formation becomes important and variations in selectivity must be accounted for. The interpretation proposed implies surface dehydration to begin at about 230°C, a considerable sharpening of the 200–300°C range for incipient dehydration quoted by McIver *et al.* (26).

**Summary correlation.** The analysis of surface hydration and adsorption competition given above may be summarized by the following computation for the rate of ether formation:

$$\frac{r}{r_0} = \exp \left[ -\frac{E}{R} \left( \frac{1}{T} - \frac{1}{T_0} \right) \right] \left[ \frac{1 - RF}{1 - RF_0} \right] \quad (2)$$

in which  $r_0$  is the rate under known conditions of surface coverage, surface hydration and temperature,  $r$  is the rate at new

conditions of these variables,  $RF$  is the reduction in surface coverage plus the change in favorability due to change in surface hydration, and  $RF_0$  is the same under known conditions. The  $RF$  quantities can be determined from the change in the water content of the catalyst, giving the surface coverage variation, and the configurational results of the Monte Carlo simulation in Figs. 8 and 9. Rates for other than pure alcohol feed are determined with the assistance of Fig. 10. The use of Eq. 2 is demonstrated by calculating  $r$  at 364.8°C (indicated point on Fig. 14), using as  $r_0$  the value 0.0341 moles/100 g of catalyst/min at 227°C, the reference point of 100% hydration and 100% surface coverage. At 364.8°C the water content of the catalyst is 2.7 g/g and the dehydration is thus  $(3.6 - 2.7)/3.6$  or 25%. This is the reduction factor for surface coverage. Referring to Fig. 8, one finds that at 75% hydration and pure alcohol feed the relative favorability is only 0.56. The calculation is, then:

$$\frac{r}{r_0} = \exp \left[ -13850 \left( \frac{1}{637.8} - \frac{1}{500} \right) \right] \times \left[ \frac{1 - (0.44 + 0.25)}{1} \right]. \quad (3)$$

Thence:

$$r = (115)(0.0341) = 3.92 \text{ moles of alcohol/min/100 g of catalyst}$$

The measured value of  $r$  is 3.12. This agreement is very good when one considers that a 100-fold range of rate is involved with the extrapolation to 365°C of the experimental error in an activation energy determined at 175–227°C.

**Activation energy for ethylene formation.**

Equation (2) can be used to eliminate the uncertainties introduced into determination of the activation energy for ethylene formation by surface dehydration and surface coverage variation. As  $r_0$  we use the measured rate for ethylene of 0.392 moles/100 g of catalyst-min at 285.4°C, surface coverage and surface hydration of 87% (calculated from ether considerations). The reduction factor in this case, computed from Fig. 9 for ethylene, is (−0.11); that is, there are more favorable sites for

ethylene as the surface is dehydrated until the maximum in Fig. 9 is attained.  $RF_0$  is  $(0.13-0.11) = 0.02$ . The results of several calculations at higher temperatures are given in Table 4. The values tabulated in

TABLE 4  
CALCULATIONS FOR DETERMINATION OF  
ACTIVATION ENERGY OF  
ETHYLENE FORMATION

$T$ (°C)	$r$	Surface hydration	$RF$	$(r/r_0)$ $(1 - RF_0/1 - RF)$
285.4	0.0392	0.87	0.02	—
352.7	1.665	0.77	0.10	1.67
358.6	2.20	0.76	0.11	1.79
364.8	4.12	0.75	0.12	2.07
391.8	6.29	0.72	0.16	2.27

the right hand column of the table, when plotted in Arrhenius form, give a straight line from which an activation energy of 29.2 kcal/g mole is computed for ethylene formation.

#### CONCLUSIONS

The success of the Monte Carlo simulation of reaction in the present study, taken together with the prior success of similar methods in simulation of surface hydration of alumina and reaction selectivity in hydrocarbon oxidation, indicates considerable potential in certain areas of modeling or simulation of catalytic behavior. To be sure, a considerable amount of information must be available concerning the surfaces and reactions involved; however, once this is provided the simulation allows systematic exploration of even rather complexly interrelated effects (as in the present case). This is hardly to say that the days of catalytic experimentation are numbered, since the basic parameters of any simulation (i.e., adsorption constants, activation energies) are experimental quantities, but applications to estimation of rates and selectivities for design may very well allow reduction of the experimental burden.

#### ACKNOWLEDGMENT

This research was supported by the National Science Foundation under Grant GK-81. The assistance of the Yale Computer Center and

Chevron Research Company in funding computer time is gratefully acknowledged.

#### REFERENCES

- HINDIN, S. G., AND WELLER, S. W., *J. Phys. Chem.* **60**, 1501 (1956).
- PINES, H., AND HAAG, W. O., *J. Amer. Chem. Soc.* **82**, 2471 (1960).
- MACIVER, D. S., WILMOT, W. H., AND BRIDGES, J. M., *J. Catal.* **3**, 502 (1964).
- HALL, W. K., LUTINSKI, F. E., AND GERBERICH, H. R., *J. Catal.* **3**, 512 (1964).
- MYERS, J. W., presented: AIChE New Orleans Meet., March, 1969.
- VERWEY, E. J. W., *Z. Kristallogr.* **91**, 65 (1935).
- LIPPENS, D. B., thesis, Technische Hogeschool, Delft, The Netherlands, 1961.
- MOLIERE, K., RATHJE, W., AND STRONSKI, I. N., *Discuss. Faraday Soc.* **5**, 21 (1961).
- TAMELE, M. W., *Discuss. Faraday Soc.* **8**, 270 (1950).
- PERI, J. B., AND HANNAN, R. B., *J. Phys. Chem.* **64**, 1526 (1960); **69**, 211, 220 (1965).
- PERI, J. B., *Actes Congr. Int. Catal. 2nd*, 1960 **1**, 1333 (1961).
- CALLAHAN, J. L., AND GRASSELLI, R. K., *AIChE J.* **9**, 755 (1963).
- WINFIELD, M. E., "Catalysis" (P. H. Emmett, ed.), Vol. 7. Reinhold, New York, 1960.
- PINES, H., AND MANASSEN, J., *Advan. Catal. Relat. Subj.* **16**, 49 (1966).
- WADE, W. H., TERANISHI, S., AND DURHAM, J. L., *J. Phys. Chem.* **69**, 590 (1965).
- ARAI, H., SAITO, Y., AND YONEDA, Y., *J. Catal.* **10**, 128 (1968).
- SOLOMON, H. J., BLISS, H., AND BUTT, J. B., *Ind. Eng. Chem. Fundam.* **6**, 325 (1967).
- KNÖZINGER, H., SCHEGLILA, A., AND WATSON, A. M., *J. Phys. Chem.* **72**, 2770 (1968).
- KNÖZINGER, H., BUHL, H., AND RESS, E., *J. Catal.* **12**, 121 (1969).
- BUTT, J. B., BLISS, H., AND WALKER, C. A., *AIChE J.* **8**, 42 (1962).
- KNÖZINGER, H., AND KOHNE, R., *J. Catal.* **3**, 559 (1964).
- DABROWSKI, J. E., PhD dissertation, Yale University, 1969.
- KIPLING, J. J., AND PEAKALL, D. B., "Chemisorption" (W. E. Graner, ed.), p. 59. Butterworths, London, 1957.
- YOSHIDA, F., RAMASWAMI, D., AND HOUGEN, O. A., *AIChE J.* **8**, 5 (1962).
- WEISZ, P. B., AND HICKS, J. S., *Chem. Eng. Sci.* **17**, 265 (1962).
- MACIVER, D. S., TOBIN, H. H., AND BARTH, R. T., *J. Catal.* **2**, 485 (1963).